Determination of the Workspace of 6-DOF Parallel Manipulators

C. Gosselin*
INRIA (Projet Prisme),
Centre de Sophia-Antipolis,
2004 Route des Lucioles,
06565 Valbonne Cedex,
France

This paper presents an algorithm for the determination of the workspace of parallel manipulators. The method described here, which is based on geometrical properties of the workspace, leads to a simple graphical representation of the regions of the three-dimensional Cartesian space that are attainable by the manipulator with a given orientation of the platform. Moreover, the volume of the workspace can be easily computed by performing an integration in its boundary, which is obtained from the algorithm. Examples are included to illustrate the application of the method to a six-degree-of-freedom fully parallel manipulator.

1 Introduction

Over the last decade, several researchers have addressed the problem of the analysis, design, and control of parallel manipulators (see for instance the references at the end of this paper). The idea behind these manipulators is that they exhibit a better rigidity—and therefore a better load-carrying capacity—than common serial manipulators. Hence, they are of great interest for applications where heavy loads or high speed and precision are needed.

MacCallion and Pham (1979) have suggested to use a parallel device as a workstation for assembly. Then, after a systematic review of the different kinematic possibilities for parallel manipulators, a few architectures of fully parallel devices emerged as the most promising designs (Hunt, 1983). These architectures have been studied in more detail by other authors. Yang and Lee (1984), Mohamed and Duffy (1985), Fichter (1986), and Merlet (1987, 1988) studied the six-degree-of-freedom fully parallel manipulator which is represented in Fig. 1. On the other hand, Gosselin and Angeles (1988, 1989) reported on the analysis and optimization of planar and spherical three-degree-of-freedom parallel manipulators whereas Lee and Shah (1988) worked on the design of a spatial three-degree-of-freedom parallel manipulator. As an alternative design, Inoue et al. (1985) have developed a six-degree-of-freedom parallel manipulator based on parallelogram mechanisms.

However, as most of the authors mentioned above have pointed out, the major drawback of parallel manipulators is their limited workspace. Hence, it is of primary importance to develop some efficient tools that will allow us to determine their workspace. Moreover, in the context of design, the workspace determination procedure should be simple enough to be included in an optimization cycle. Asada and Youcef-Toumi (1984) and Bajpai and Roth (1986) have studied the reachable workspace of a closed-loop planar two-degree-of-freedom manipulator using the kinematic equations of planar five-bar mechanisms and Gosselin and Angeles (1988, 1989) have used geometric considerations to evaluate and optimize the workspace of planar and spherical three-degree-of-freedom manipulators. However, the workspace of spatial six-degree-of-freedom parallel manipulators has been described only through methods based on a complete discretization of the Cartesian space (Yang and Lee, 1984; Fichter, 1986; Merlet, 1987, 1988).

In this paper, sections of the workspace of six-degree-of-freedom parallel manipulators are obtained geometrically. Since the workspace of a six-degree-of-freedom manipulator is embedded in a six-dimensional space, it is very difficult to represent. The workspace determined here is the positioning workspace, i.e., the region of the three-dimensional Cartesian space that can be attained by the manipulator with a given orientation of the platform. This is in fact a three-dimensional section of the six-dimensional workspace but any of these sections can be obtained with the method described here. First of all, the inverse kinematic problem of a parallel manipulator is considered and its solution, which was derived somewhere else, is used to establish regions in space whose intersection will result in the workspace. Then, an algorithm for the computation of that intersection is developed and extended to

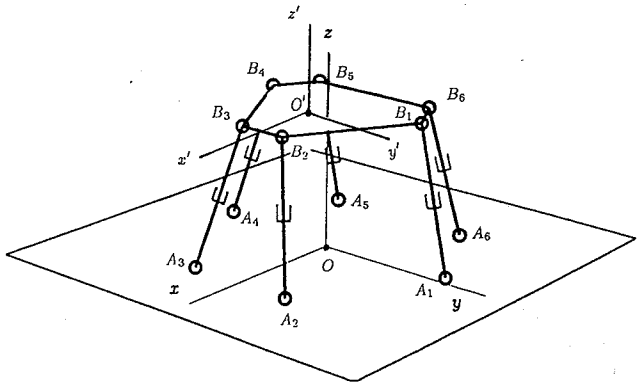

Fig. 1 Spatial six-degree-of-freedom parallel manipulator

*Currently at Université Laval, Département de Génie Mécanique, Québec, Canada.

Contributed by the Mechanisms Committee for publication in the JOURNAL OF MECHANICAL DESIGN. Manuscript received May 1989.

include the computation of the volume of the workspace. Finally, an example of application of the method to the INRIA prototype will be presented.

2 Inverse Kinematics

The solution of the inverse kinematic problem is now rederived in order to clearly establish the notation used here. Let us consider a fixed coordinate frame $R : O - xyz$ attached to the base of the manipulator and a moving coordinate frame $R' : O' - x'y'z'$ attached to the platform, where O' is the point to be positioned by the manipulator (Fig. 1). Moreover, the center of the joint connecting the ith leg to the base will be denoted as A_i whereas the center of the joint connecting the same leg to the platform will be denoted as B_i. Therefore, vectors $(\mathbf{a}_i,\ i = 1, \ldots, 6)$, will be defined as the position vectors of the base joints, which are constant vectors when expressed in frame R, and vectors $(\mathbf{b}_i,\ i = 1, \ldots, 6)$ will be defined as the position vectors of the platform joints, which are constant when expressed in frame R'. Furthermore, let $\mathbf{Q}$ be the rotation matrix describing the orientation of R' with respect to R, i.e., the orientation of the platform with respect to the base, and let ρ_i be the length of the ith leg. If the position of point O' with respect to the origin of the fixed coordinate frame R is denoted by vector $[\mathbf{r}]_R = [x_r, y_r, z_r]^T$, we can write

$$[\mathbf{b}_i]_R = [\mathbf{r}]_R + \mathbf{Q}[\mathbf{b}_i]_{R'}, \quad i = 1, \ldots, 6] \tag{1}$$

where the subscript outside of the brackets indicates in which coordinate frame the vector is expressed. Now, subtracting vector $\mathbf{a}_i$ from both sides of equation (1) leads to

$$[\mathbf{b}_i - \mathbf{a}_i]_R = [\mathbf{r}]_R + \mathbf{Q}[\mathbf{b}_i]_{R'} - [\mathbf{a}_i]_R, \quad i = 1, \ldots, 6 \tag{2}$$

The left-hand side of equation (2) is clearly the vector—along the ith leg—connecting point A_i to point B_i and, therefore, by taking the Euclidean norm of each side of equation (2), we obtain

$$\rho_i = \| [\mathbf{b}_i - \mathbf{a}_i]_R \| = \| [\mathbf{r}]_R + \mathbf{Q}[\mathbf{b}_i]_{R'} - [\mathbf{a}_i]_R \|, \quad i = 1, \ldots, 6 \tag{3}$$

Hence, for given values of the positions of the joints on the base and on the platform, i.e., for a given manipulator, and for prescribed values of the position and orientation of the platform, the required actuator lengths can be directly computed from equation (3) which is in fact the solution of the inverse kinematic problem. In scalar form, equation (3) can be rewritten as

$$\rho_i^2 = (x_r - u_i)^2 + (y_r - v_i)^2 + (z_r - w_i)^2, \quad i = 1, \ldots, 6 \tag{4}$$

where

$$u_i = x_{ai} - q_{11}x_{bi} - q_{12}y_{bi} - q_{13}z_{bi}, \quad i = 1, \ldots, 6 \tag{5}$$

$$v_i = y_{ai} - q_{21}x_{bi} - q_{22}y_{bi} - q_{23}z_{bi}, \quad i = 1, \ldots, 6 \tag{6}$$

$$w_i = z_{ai} - q_{31}x_{bi} - q_{32}y_{bi} - q_{33}z_{bi}, \quad i = 1, \ldots, 6 \tag{7}$$

where q_{ij} stands for the (i,j) entry of the rotation matrix $\mathbf{Q}$, and where the components used in equations (5–7) are defined as:

$$[\mathbf{a}_i]_R = [x_{ai}, y_{ai}, z_{ai}]^T, \quad i = 1, \ldots, 6 \tag{8}$$

$$[\mathbf{b}_i]_{R'} = [x_{bi}, y_{bi}, z_{bi}]^T, \quad i = 1, \ldots, 6 \tag{9}$$

3 Geometric Description of the Workspace

The solution of the inverse kinematic problem developed above can be used to describe the workspace of the parallel manipulator. Indeed, if mechanical interferences are neglected, the boundary of the workspace is attained whenever at least one of the actuators reaches one of its limits. If we assume that the range of motion of the actuators is given by

$$\rho_{\min} < \rho_i < \rho_{\max}, \quad i = 1, \ldots, 6 \tag{10}$$

then the boundary of the workspace can be described as the set of points for which we have

$$\rho_i = \rho_{\min} \quad \text{or} \quad \rho_i = \rho_{\max} \tag{11}$$

for at least one of the legs while all other actuators have lengths that are within their range of motion. Using the development of section 2, we can rewrite condition (11) as:

$$(x_r - u_i)^2 + (y_r - v_i)^2 + (z_r - w_i)^2 = \rho_{\min}^2 \tag{12}$$

or

$$(x_r - u_i)^2 + (y_r - v_i)^2 + (z_r - w_i)^2 = \rho_{\max}^2 \tag{13}$$

Moreover, for a given orientation of the platform, i.e., for a specified matrix $\mathbf{Q}$, quantities u_i, v_i, and w_i become constant and equations (12) and (13) represent concentric spheres of radii $\rho_{\min}$ and $\rho_{\max}$, respectively, which circumscribe the portion of the three-dimensional Cartesian space attainable by the ith leg. However, it is pointed out that the center of the spheres, given by point $C_i\ (u_i, v_i, w_i)$ does not coincide with the center of the joint connecting the ith leg to the base, but is rather given by:

$$\begin{bmatrix} u_i \\ v_i \\ w_i \end{bmatrix} = [\mathbf{a}_i]_R - [\mathbf{b}_i]_R = [\mathbf{a}_i]_R - \mathbf{Q}[\mathbf{b}_i]_{R'}, \quad i = 1, \ldots, 6 \tag{14}$$

This is so because the description of the workspace given by equations (12) and (13) has to take into account the geometry of the platform. In other words, the concentric spheres represent the trajectory described by point O' of the platform when the ith leg, with minimum or maximum extension, is rotated about its fixed spherical joint—located at point A_i—while the attitude of the platform is maintained unchanged. Therefore, vector $[\mathbf{b}_i]_R$ has to be subtracted from $[\mathbf{a}_i]_R$, as shown in Fig. 2, in order to obtain the center of the sphere C_i. The smaller sphere is obtained with $\rho_i = \rho_{\min}$ and the larger one with $\rho_i = \rho_{\max}$. Hence, for a given orientation of the platform, the workspace of the parallel manipulator in three-dimensional Cartesian space can be described as the intersection of 6 regions, each of these regions being the difference of two concentric spheres. The position of the centers of the spheres will depend on the kinematic parameters of the manipulator and on the orientation specified for the platform.

A section of the workspace can then be obtained by taking a section of the spheres described above, i.e., by taking the intersection of the spheres with a plane. This will lead to 6 pairs of concentric circles. For instance, if it is desired to find

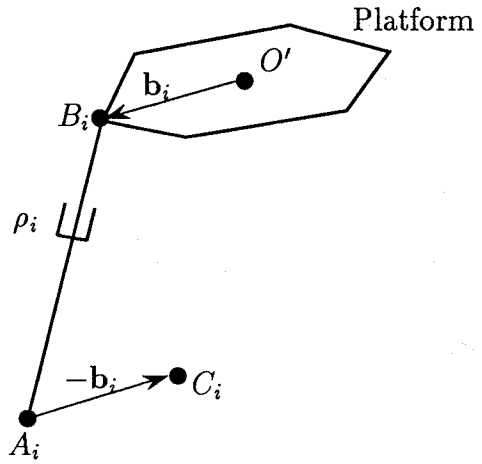

Fig. 2 Location of the center of each of the spheres used to compute the workspace

the section of the workspace on a plane parallel to the xy plane, defined as $z = z_H$, then equations (12) and (13) are rewritten as:

$$(x_r-u_i)^2+(y_r-v_i)^2=R^2_{\min,i} \tag{15}$$

$$(x_r-u_i)^2+(y_r-v_i)^2=R^2_{\max,i} \tag{16}$$

where we have

$$R^2_{\min,i}=\begin{cases}\rho^2_{\min}-(z_H-w_i)^2, & \text{if } \rho^2_{\min}-(z_H-w_i)^2>0\\ 0, & \text{otherwise}\end{cases} \tag{17}$$

and

$$R^2_{\max,i}=\begin{cases}\rho^2_{\max}-(z_H-w_i)^2, & \text{if } \rho^2_{\max}-(z_H-w_i)^2>0\\ 0, & \text{otherwise}\end{cases} \tag{18}$$

The radii of the concentric circles are given by $R_{\min,i}$ and $R_{\max,i}$ respectively. It is to be noted that the condition in equations (17) and (18) is introduced to take into account the cases for which the sphere does not intersect the given plane.

Similarly, if the section of the workspace on a plane parallel to the xz plane, defined as $y = y_H$, is to be obtained, then equations (12) and (13) can now be rewritten as:

$$(x_r-u_i)^2+(z_r-w_i)^2=R^2_{\min,i} \tag{19}$$

$$(x_r-u_i)^2+(z_r-w_i)^2=R^2_{\max,i} \tag{20}$$

where we have, in that case

$$R^2_{\min,i}=\begin{cases}\rho^2_{\min}-(y_H-v_i)^2, & \text{if } \rho^2_{\min}-(y_H-v_i)^2>0\\ 0, & \text{otherwise}\end{cases} \tag{21}$$

and

$$R^2_{\max,i}=\begin{cases}\rho^2_{\max}-(y_H-v_i)^2, & \text{if } \rho^2_{\max}-(y_H-v_i)^2>0\\ 0, & \text{otherwise}\end{cases} \tag{22}$$

A section of the workspace can therefore be determined by finding the intersection of 6 annular regions, i.e., six regions defined as the difference between two concentric circles. An algorithm for the solution of this problem is proposed in the next section.

4 Algorithm for Workspace Evaluation

The intersection of the 6 annular regions described above can be obtained geometrically. Two important observations concerning the characteristics of the workspace of the parallel manipulator have to be made at this point.

Observation 1: Since the workspace in three-dimensional Cartesian space is obtained by the intersection of regions bounded by spheres, we can conclude that the boundary of the workspace will consist exclusively in a set of portions of spheres.

Observation 2: The second observation follows from the first one. Indeed, since a section of the workspace is obtained by the intersection of regions bounded by circles, then the boundary of that section will be made up of circular arcs, i.e., portions of circles.

The algorithm that is now described is based on the second observation. The procedure followed to obtain the section of the workspace on planes parallel to the xy plane is presented.

As discussed in the previous section, if the section on a plane parallel to the xy plane is needed, equations (12) and (13) are rewritten as equations (15) and (16) which represent circles in the plane of the section. Therefore, the problem is now to find the intersection of the 6 annular regions. As stated in observation 2, the boundary of this intersection will consist in a series of circular arcs connected to each other. It is possible to identify the arcs that are potential candidates for a portion of the boundary of the workspace by computing the intersection of each of the circles with all the other ones. This is the first step of the algorithm.

STEP 1: For each of the circles described in equations (15) and (16), find all the intersections with the other circles.

Computing the intersection of two distinct circles is a straightforward procedure which can yield to 0,1 or 2 solutions. Once all the intersection points are obtained, they have to be ordered so that each circle is divided in a set of circular arcs. If no intersection is found on a particular circle, it is represented as only one circular arc, i.e., the circle itself. The second step can be stated as:

STEP 2: Obtain all the circular arcs defined by the intersection points found on the circles by ordering these points.

Now, since all the circular arcs found in the previous step will not be part of the boundary of the workspace, we have to use a checking procedure to identify the arcs that constitute the boundary of the workspace. The following test, which is based on equation (11) and the condition attached to it, is used: for a given arc, belonging to a given circle, we choose a point lying on the arc—preferably not one of the end points—and check whether or not this point is located inside all the other external circles and outside all the other internal circles. The terms internal and external circles refer to the inner and outer limits of each of the annular regions. In other words, the circle to which the arc belongs is eliminated and the test is performed on the 11 other circles. Clearly, when the arc is within all the outer circles and outside of all the inner circles, it constitutes part of the boundary of the workspace. This test is equivalent to the condition attached to equation (11), i.e., that all the actuators have lengths within their range of motion. If the test fails, then the arc is rejected. Step 3 of the algorithm then becomes:

STEP 3: Perform a test on each of the circular arcs identified in step 2 in order to determine which ones constitute the boundary of the workspace. The test consists in checking if the arc—one point on it will be used in practice—is within all the other outer circles and outside all the other inner circles.

When these operations are completed, we have a list of circular arcs which constitute the boundary of the workspace. Some of these arcs may be portions of inner circles whereas others may be portions of outer circles. It is pointed out that the procedure described above for finding sections of the workspace on planes parallel to the xy plane is also applicable to the determination of the sections on other planes. For example, sections on planes parallel to the xz plane are obtained by using equations (19) and (20) instead of equations (15) and (16).

The next problem to be addressed is the computation of the area of the sections of the workspace. Since we have an accurate description of the boundary of the workspace, i.e., the list of circular arcs obtained above, it is natural to determine the area by performing the integration on the boundary. This technique was used in Gosselin and Angeles (1988) to compute the volume of the workspace of a planar manipulator. It is based on the Gauss Divergence Theorem (Brand, 1955), which can be applied to planar regions to give:

$$A=\frac{1}{2}\int_{\partial\Omega}\mathbf{s}\cdot\mathbf{n}\,d\partial\Omega \tag{23}$$

where

A = area of the planar region

$\partial\Omega$ = the boundary of the planar region

$\mathbf{s}$ = the position vector of an arbitrary point of $\partial\Omega$

$\mathbf{n}$ = the outward unit normal vector to the curve $\partial\Omega$

In the present case, since the workspace is described as a series of circular arcs, equation (23) can be rewritten as:

Table 1 Geometric properties of the INRIA prototype (all lengths are given in mm)

i	1	2	3	4	5	6
x_{ai}	92.58	132.58	40.00	-40.00	-132.58	-92.58
y_{ai}	99.64	30.36	-130.00	-130.00	30.36	99.64
z_{ai}	23.10	23.10	23.10	23.10	23.10	23.10
x_{bi}	30.00	78.22	48.22	-48.22	-78.22	-30.00
y_{bi}	73.00	-10.52	-62.48	-62.48	-10.52	73.00
z_{bi}	-37.10	-37.10	-37.10	-37.10	-37.10	-37.10
$s_{i\min}$	454.5	454.5	454.5	454.5	454.5	454.5
$s_{i\max}$	504.5	504.5	504.5	504.5	504.5	504.5

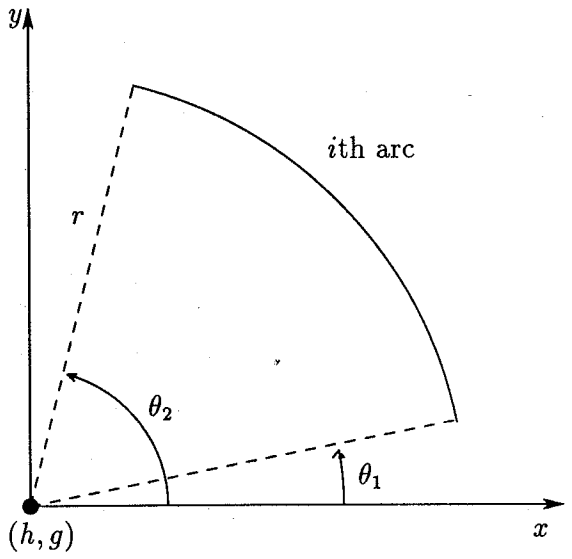

Fig. 3 Geometric description of the *i*th arc

$$A=\frac{1}{2}\sum_{i=1}^{N_a}A_i \tag{24}$$

with

$$A_i=\int_{\partial\Omega_i}\mathbf{s}\cdot\mathbf{n}\,d\partial\Omega_i \tag{25}$$

where N_a is the number of arcs constituting the boundary of the workspace and $\partial\Omega_i$ is now the *i*th circular arc. Moreover, if the *i*th arc is described as shown in Fig. 3, i.e., using the position of its center of curvature given by vector $[h, g]^T$, its radius of curvature r, and the angles corresponding to the end points, given by θ_1 and θ_2, respectively, using a counterclockwise convention, and with respect to a fixed coordinate frame $O-xy$, then vectors $\mathbf{s}$ and $\mathbf{n}$ can be written as:

$$\mathbf{s}=\begin{bmatrix}h\\g\end{bmatrix}+\begin{bmatrix}r\cos\theta\\r\sin\theta\end{bmatrix} \tag{26}$$

and

$$\mathbf{n}=\begin{cases}[\cos\theta, \sin\theta]^T, & \text{if the arc is on an outer circle}\\ [-\cos\theta, -\sin\theta]^T, & \text{if the arc is on an inner circle}\end{cases} \tag{27}$$

This is so because the normal vector $\mathbf{n}$, as defined in equation (23) has to be pointing towards the outside of the area of interest. Hence, by substituting equations (26) and (27) in equation (25), we get:

$$A_i=gr[\sin\theta_2-\sin\theta_1]+hr[\cos\theta_2-\cos\theta_1]+r^2[\theta_2-\theta_1] \tag{28}$$

for an outer circle and

$$A_i=-gr[\sin\theta_2-\sin\theta_1]-hr[\cos\theta_2-\cos\theta_1]-r^2[\theta_2-\theta_1] \tag{29}$$

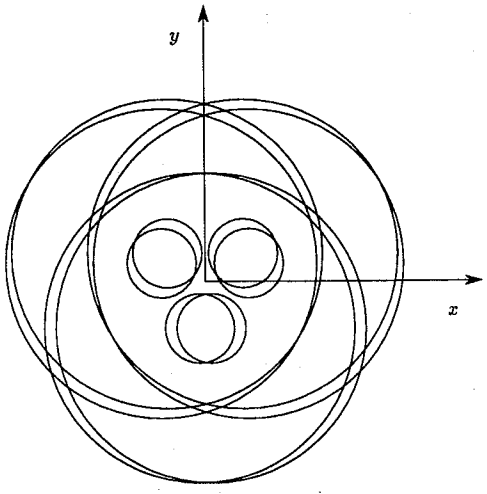

Fig. 4 The 6 pairs of concentric circles defined by equations (15) and (16) for z = 512 mm

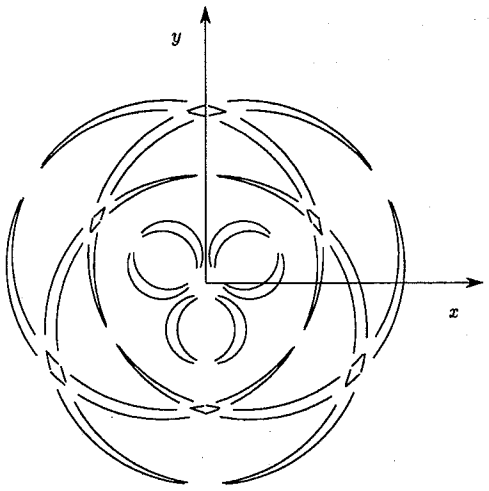

Fig. 5 The circles of Fig. 4 are divided in a series of circular arcs

for an inner circle. It is recalled from above that θ_1 and θ_2 are the angles corresponding to the beginning and end points of the given arc. This computation is easily included in the algorithm described above. Indeed, when a circular arc is declared valid by the test performed in step 3 of the algorithm, one only has to compute its contribution to the area by using either equation (28) or equation (29). The summation of all the contributions as shown in equation (24) will yield the area of the section of the workspace.

When the above procedure is repeated for a series of parallel planes, for instance planes parallel to the xy plane, the volume of the workspace in the xyz space can be obtained by using any appropriate quadrature rule to numerically integrate the area of the "slices" of the workspace obtained above.

5 Example

As an example of application of the algorithm described above, the workspace of the parallel manipulator developed at INRIA will now be studied. The INRIA prototype, which is a six-degree-of-freedom fully parallel manipulator, was described in detail in (Merlet, 1987, 1988). Its geometric properties are summarized in Table 1. Equations (15) and (16) were used here to obtain a geometric description of some sections of the workspace parallel to the xy plane for a reference orientation of the platform, i.e., when $\mathbf{Q} = \mathbf{1}$, where $\mathbf{1}$ is the identity matrix.

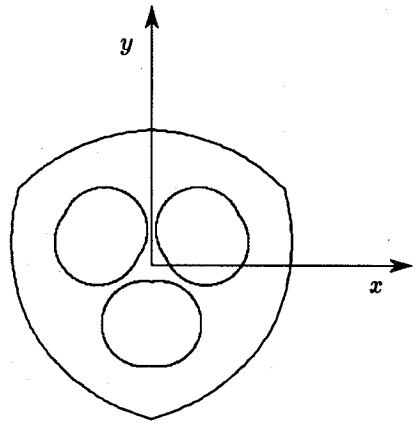

Area=55168 mm^2

Fig. 6 Boundary of the workspace for z = 512 mm

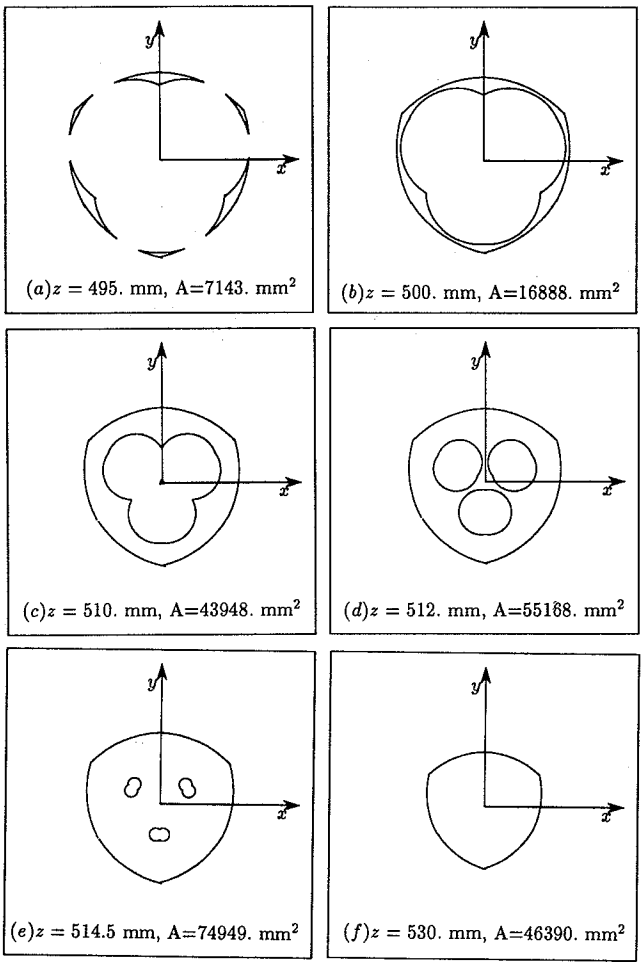

Fig. 7 Boundary of the workspace for different values of z, i.e., sections of the workspace in planes parallel to the xy plane

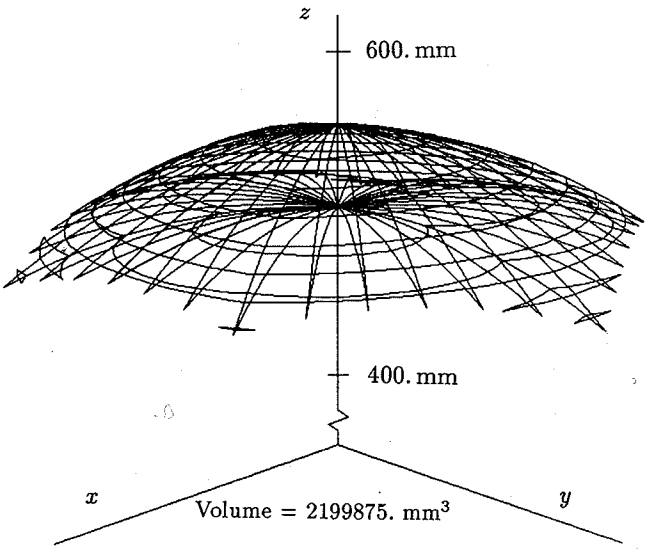

Fig. 8 Spatial representation of the workspace of the INRIA parallel manipulator for the reference orientation of the platform

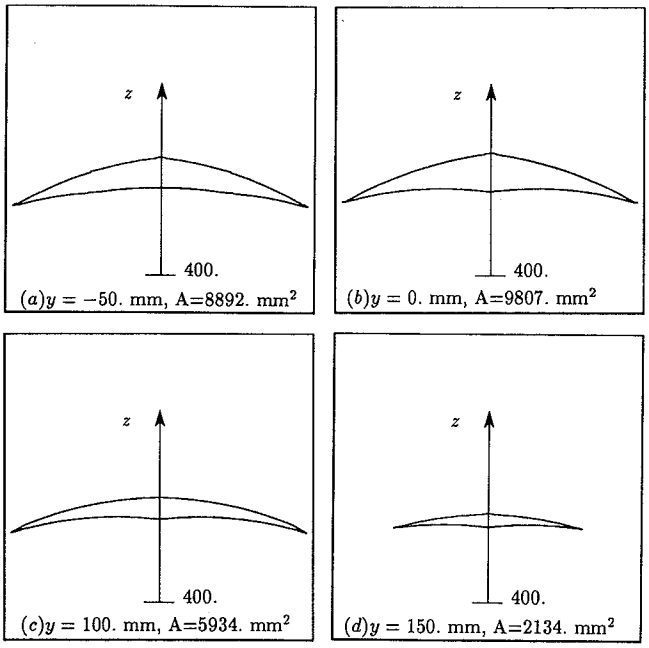

Fig. 9 Sections of the workspace in planes parallel to the xz plane

For instance, when z is equal to 512 mm, the circles described by equation (15) and (16) are as shown in Fig. 4. Next, using the algorithm of section 4, we divide the circles in a series of circular arcs by computation of the intersection points of the circles. This is schematically represented in Fig. 5. Then by elimination of the irrelevant arcs, we obtain the boundary of the workspace, which is shown in Fig. 6. The zones where the 6 annular regions intersect have then been found. Also, the contribution of each of the arcs to the area of the section of the workspace has been computed and added up to lead the total area.

A similar procedure is followed for several values of z. A few sections are illustrated in Fig. 7 where the areas are also indicated. Using the different sections, a representation of the volume of the workspace in the xyz space for the reference orientation of the platform is obtained as shown in Fig. 8. In that figure, the sections in planes parallel to the xy plane have been used together with sections in a series of vertical planes intersecting the z axis in order to obtain a better representation. The global shape of the workspace is that of an umbrella. Moreover, the sections in planes parallel to the xy plane described above clearly indicate that, for a given value of z, there may exist some regions of the plane within the external boundary of the workspace that cannot be reached. For the reference

orientation, the volume of the workspace of the INRIA prorotype is equal to approximately 2.2×10^6 mm^3.

Using equations (19) and (20), sections of the workspace on planes parallel to the xz plane have been obtained. A few of them are shown in Fig. 9 with the corresponding values for the areas.

6 Conclusion

An algorithm for the determination of three-dimensional sections of the workspace of parallel manipulators has been presented in this paper. The algorithm is based on the geometric description of the boundaries of the workspace, which was shown to be obtained from the intersection of 6 regions, each of which being the difference between two concentric spheres. The problem was then reduced to a two-dimensional one by considering planar sections of the workspace. The boundary of the workspace was therefore represented as a set of circular arcs on these sections and a method of integration on the boundary was used to determine the volume of the workspace. An example of application to the INRIA prototype was presented which led to an accurate representation of the workspace. Moreover, the evaluation of the volume of the reachable portion of the space can be performed at a reasonable cost which is an important issue in the context of design and optimization.

7 Acknowledgments

The research work reported here was completed under a post-doctorate scholarship granted to the author by the French Government.

8 References

Asada, H., and Youcef-Toumi, K., 1984, "Analysis and Design of a Direct-Drive Arm With a Five-Bar-Link Parallel Drive Mechanism," ASME *Journal of Dynamic Systems, Measurements, and Control*, Vol. 106, No. 3, pp. 225–230.

Bajpai, A., and Roth, B., 1986, "Workspace and Mobility of a Closed-Loop Manipulator," *The International Journal of Robotics Research*, Vol. 5, No. 2, pp. 131–142.

Brand, L., 1955, *Advanced Calculus*, John Wiley, New York, pp. 355–361.

Fichter, E. F., 1986, "A Stewart Platform-Based Manipulator: General Theory and Practical Construction," *The International Journal of Robotics Research*, Vol. 5, No. 2, pp. 157–182.

Gosselin, C., and Angeles, J., 1988, "The Optimum Kinematic Design of a Planar Three-Degree-of-Freedom Parallel Manipulator," ASME JOURNAL OF MECHANISMS, TRANSMISSIONS, AND AUTOMATION IN DESIGN, Vol. 110, No. 1, pp. 35–41.

Gosselin, C., and Angeles, J., 1989, "The Optimum Kinematic Design of a Spherical Three-Degree-of-Freedom Parallel Manipulator," ASME JOURNAL OF MECHANISMS, TRANSMISSIONS, AND AUTOMATION IN DESIGN, Vol. 111, No. 2, pp. 202–207.

Hunt, K. H., 1983, "Structural Kinematics of In-Parallel-Actuated Robot Arms," ASME JOURNAL OF MECHANISMS, TRANSMISSIONS, AND AUTOMATION IN DESIGN, Vol. 105, No. 4, pp. 705–712.

Inoue, H., Tsusaka, Y., and Fukuizumi, T., 1985, "Parallel Manipulator," *Proceedings of the 3rd International Symposium on Robotics Research*, October 7–11, Gouvieux, France, pp. 321–327.

Lee, K. M., and Shah, D. K., 1988, "Kinematic Analysis of a Three-Degree-of-Freedom In-Parallel Actuated Manipulator," *IEEE Journal of Robotics and Automation*, Vol. 4, No. 3, pp. 354–360.

MacCallion, H., and Pham, D. T., 1979, "The Analysis of a Six Degree of Freedom Work Station for Mechanised Assembly," *Proceedings of the 5th World Congress on Theory of Machines and Mechanisms*, July, Montréal.

Merlet, J. P., 1987,"Parallel Manipulators, Part I: Theory, Design, Kinematics, Dynamics and Control," Technical Report No. 646 INRIA, France.

Merlet, J. P., 1988, "Force-Feedback Control of Parallel Manipulators," *Proceedings of the IEEE International Conference on Robotics and Automation*, Philadelphia April 24–29, pp. 1484–1489.

Mohamed, M. G., and Duffy, J., 1985, "A Direct Determination of the Instantaneous Kinematics of Fully Parallel Robot Manipulators," ASME JOURNAL OF MECHANISMS, TRANSMISSIONS, AND AUTOMATION IN DESIGN, Vol. 107, No. 2, pp. 226–229.

Yang, D. C. H., and Lee, T. W., 1984, "Feasibility Study of a Platform Type of Robotic Manipulators from a Kinematic Viewpoint," ASME JOURNAL OF MECHANISMS, TRANSMISSIONS, AND AUTOMATION IN DESIGN, Vol. 106, No. 2, pp. 191–198.